Toward Autonomous Cardiac Catheterization Through a Parametric Finite Element Simulation With Experimental Validation

Majid Roshanfar
Department of Mechanical Engineering
Concordia University
Montreal, Canada
e-mail: m_roshan@encs.concordia.ca

Pedram Fekri
Department of Mechanical Engineering
Concordia University
Montreal, Canada
e-mail: p_fekri@encs.concordia.ca

Javad Dargahi
Department of Mechanical Engineering
Concordia University
Montreal, Canada
e-mail: dargahi@encs.concordia.ca

***Abstract*—Catheters are thin tubes or wires made of medical-grade materials that are inserted through small incisions into the human body. In order to have a safe and effective robot-assisted radio frequency ablation, a real-time force estimator is required to measure the applied forces at the tip of the catheter. Finite element analysis can provide the real-time contact force of the steerable catheter. To do so, a nonlinear planar finite element model of the steerable catheter was first developed using parametric material properties in ANSYS software. After that, a series of finite element simulations based on each mechanical property was performed, and the deformed shape of the catheter was recorded. Next, the performance was validated by comparing the outputs of the simulation with experimental results from setup. In fact, the validation force was between the range 0 and 0.45 N that determined the material properties of the catheter. The results of the proposed finite element model were in fair agreement with reference values from the experiment. The proposed method met the requirements for autonomous cardiac ablation in terms of accuracy and speed.**

***Index Terms*—Autonomous Catheterization; Finite Element Analysis; Steerable Catheter; Radio Frequency Ablation; Parametric Simulation.**

I. Introduction

In the elderly population, Atrial Fibrillation (AFib) is the most common arrhythmia, in which the electrical activity within the atria becomes chaotic [1]. Consequently, chaotic contractions of the atrium may result in blood clots and strokes [2]. As a treatment, in Radio Frequency Ablation (RFA), the arrhythmogenic sites within the cardiac tissue are partially burned off to reduce the undesired pulsation within the cardiac tissue. Catheters are thin tubes made of medical-grade materials that are inserted through small incisions into the body. The majority of atrial ablation procedures are carried out using manual catheters; however, robotic catheter intervention systems have been introduced to enable more precise mapping and ablation procedures [3][4]. It has been shown that excessive contact force (greater than 0.45 N) increases the incidence of tissue perforation, while inadequate force (less than 0.1 N) results in ineffective ablation. Figure 1 shows a scheme of a cardiac steerable RFA catheter used for AFib treatment. For RFA catheters, researchers have proposed

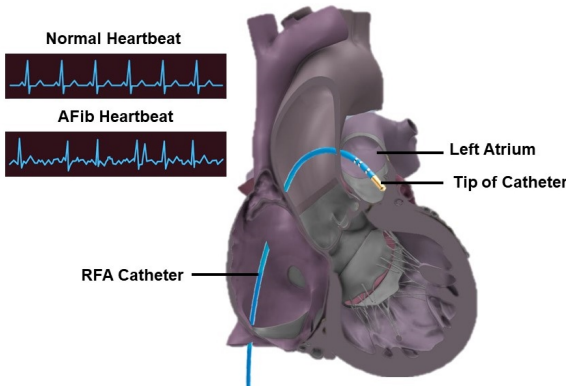

Fig. 1. Configuration of a typical ablation's catheter during an RFA procedure and a comparison of normal and arrhythmic cardiac electrical activity. (3D Heart model from Zygote Media Group Inc.)

sensor-based [5][6], and model-based [3] shape estimation schemes [7]. Even though sensor-based studies have shown favorable accuracy [8][9][10], sensor-embedded catheters are limited by their size, weight, compromised flexibility, and high cost [11]. In the literature, sensor-free approaches for estimating force have been proposed based on shape sensing [12]. Typically, these methods use real-time images of a deflected catheter to determine tip contact forces based on a mechanistic model of the catheter. Among the mechanistic methods to model the catheter is the Pseudo-Rigid-Body (PRB) model, which showed low accuracy [13][14] to be used in the medical applications. Also, the other models such as interaction modeling [15], piecewise circular arcs [16], spatial curves [17], Kirchhoff models [18], and Cosserat rod models [19][20], are not suitable for estimating the shape of the catheter in real-time because they are mainly computationally expensive. On the other hand, learning-based methods have been proposed to estimate the contact forces directly from the images containing the deflection shapes of the distal shaft [21] [22]. However, such approaches are in need to be fed by the realistic data obtained from experimental setups. Compiling a dataset that comprises all possible deflections with respect

 ISBN: 978-1-68558-053-7

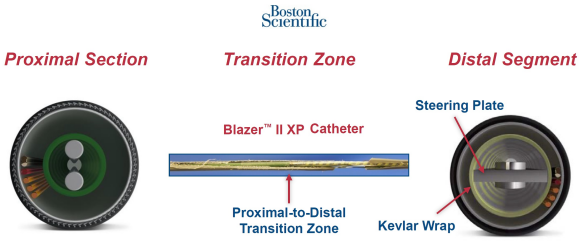

Fig. 2. Cross-section of the steerable catheter, Blazer II XP, Model 4770THK2, Boston Scientific [23].

to the eclectic catheter's material is costly and cumbersome. The scientific achievement of this study is the development of a real-time force estimator for robot-assisted radio frequency ablation using finite element analysis.

Given the reviewed limitations, this study proposes a parametric Finite Element Model (FEM) to simulate the deformation of a steerable catheter and estimate the tip contact force. The main contribution of this study is to propose a shape-based force estimation according to the finite element simulation. Due to the availability of real-time X-ray images during RFA procedures (fluoroscopy), the shape of the RFA catheter is available intraoperatively. Given such a capability, the proposed simulation can pave the way for leveraging the deep learning potentiality in finding the relationship between the parameters and their corresponding bending shape. This will obviate the run-time issue in the simulation-based approaches. Having a precise shape of the catheter along with the generated contact force outputted by the proposed simulation, it will also be possible to estimate the contact forces using the proposed method by matching the authentic catheter's deflection to the simulation output. Section II describes the finite element model used in this study. In Section III, validation of the simulation using the experimental setup will be presented and the results of the model are shown in Section IV. Finlay, the main contributions of this study will be concluded in Section V.

II. Finite Element Simulation

In this study, the catheter is modeled as a cantilever beam with a length of $L = 108$ mm and diameter $D = 2.33$ mm (this size is equivalent to the French size 7). These are the dimensions of the available catheter (Blazer II XP, Model 4770THK2, total length 110 cm, Boston Scientific [23]). Only the distal segment of the catheter was imported into the simulation. Figure 2 shows the cross-section of the proximal section and distal segment of the catheter. Since different materials are used to prototype the catheter (e.g., kevlar wrap and steering plate), the equivalent Young's modulus, Poisson's ratio and density are considered as parameters in the finite element simulations of the catheter. Then based on the deformation of the catheter during the experimental setup, the values for these parameters are tuned. During the simulation, the catheter's tip was squeezed on a rigid surface (e.g., the lumens or cardiac tissues) for 40 mm, and the reaction force at the base was recorded. Figure 3 shows the FE homogeneous Dirichlet and

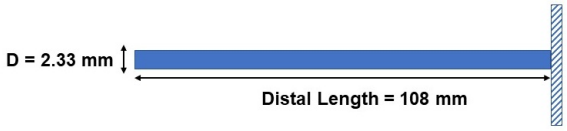

Fig. 3. Cantilever condition for the distal shaft of the catheter.

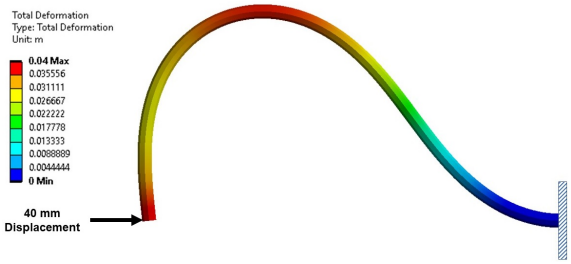

Fig. 4. Deformed shape of the catheter under 40 mm tip displacement.

Neumann boundary conditions which were applied at the rightmost of the model to simulate the cantilever condition for the distal shaft of the catheter. The model was discretized and solved using 108 elements and the nonlinear geometry (large deformation) assumption using ANSYS software (ANSYS Inc., PA, USA). Figure 4 shows the representative deformed shape of the catheter under 40 mm tip displacement. Next section will provide more details of the simulations validation.

III. Validation Study

To validate the parametric simulation and find the material properties, a range for every three parameters is considered as follows: Young's modulus ranges from 120 to 200 MPa, Poisson's ratio from 0.3 to 0.4, and density from 7000 to 8000 kg/m^3. The range specifies the minimum and maximum of each parameter during the simulation. Table I shows the experimental points for the range of each parameter and the corresponding reaction force.

TABLE I
Parametric Study Experiment Points

Experiment Points	Density (kg/m^3)	Young's Modulus (MPa)	Poisson Ratio	Reaction Force (N)
1	7500	160	0.35	0.4882
2	7000	160	0.35	0.4881
3	8000	160	0.35	0.4884
4	7500	120	0.35	0.3669
5	7500	200	0.35	0.6096
6	7500	160	0.3	0.4883
7	7500	160	0.4	0.4882
8	7093.48	127.47	0.31	0.3895
9	7906.51	127.47	0.31	0.3898
10	7093.48	192.52	0.31	0.5868
11	7906.51	192.52	0.31	0.5871
12	7093.48	127.47	0.39	0.3894
13	7906.51	127.47	0.39	0.3897
14	7093.48	192.52	0.39	0.5867
15	7906.51	192.52	0.39	0.5870

 ISBN: 978-1-68558-053-7

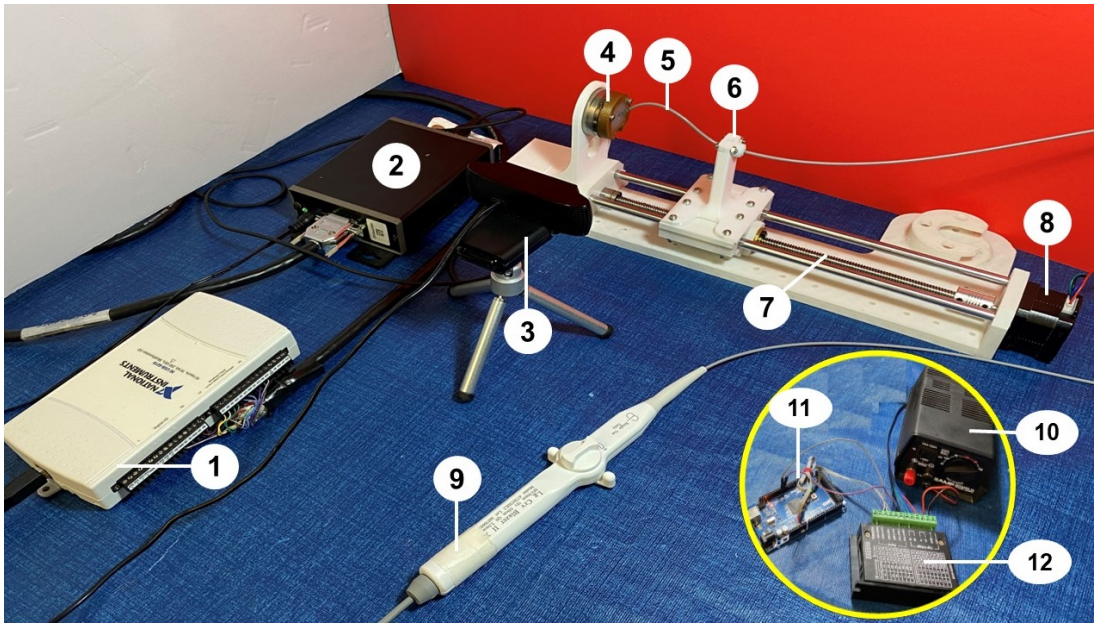

Fig. 5. Experimental setup, (1) data acquisition unit [24] (2) power supply of sensor [24] (3) camera (4) ATI Industrial Automation, F/T Sensor: Mini40 [24] (5) tip of the catheter (6) holder (7) linear actuator (8) Nema 17 stepper motor (9) steerable catheter, Blazer II XP, Model 4770THK2, Boston Scientific [23] (10) power supply (11) Arduino MEGA 2560 (12) microstep driver.

The experimental setup in Figure 5 mimics the catheter simulation. Prior to the experiment, 108 mm length of the catheter tip was measured and fixed in the holder of the linear actuator. The linear actuator was rapidly prototyped using a 3D printer (Replicator+, MakerBot, NY, USA) so as to align the center of the holder and 6-DoF force/torque sensor (ATI Industrial Automation, F/T Sensor: Mini40) (Figure 5 (4)) [24]. The purpose of the 6-DoF force/torque sensor is to measure the force applied to the clamped base by the tip of the catheter. Next, a Nema 17 stepper motor (Figure 5 (8)) controlled by an Arduino MEGA 2560 (Figure 5 (11)) squeezed the catheter tip against the force sensor mounted at the end of the linear actuator. It is the purpose of the stepper motor to drive the linear actuator. Simultaneously, a camera (Figure 5 (3)) perpendicular to the deflection plane was used to record the deflection of the catheter. During the experiment, the catheter tip's bending angle was set to 0° by using the catheter's knob, and also the initial shape of the catheter was straight. The wiring of the stepper motor in Figure 5 (8) is connected microstep driver Figure 5 (12). Figure 6 compares the result of the experiment and simulation when the tip of the catheter was squeezed for 40 mm. Utilizing ANSYS's response surface optimization (RSO) module, the candidate point is selected with the aim of minimizing the error between the reaction force obtained from the force sensor and the simulation. Figure 7 shows the recorded force during the experiment. Next section provides the result and discussion of the study.

IV. Result And Discussion

Table II shows the candidate values for the Young's modulus, Poisson ratio and density of the catheter found using

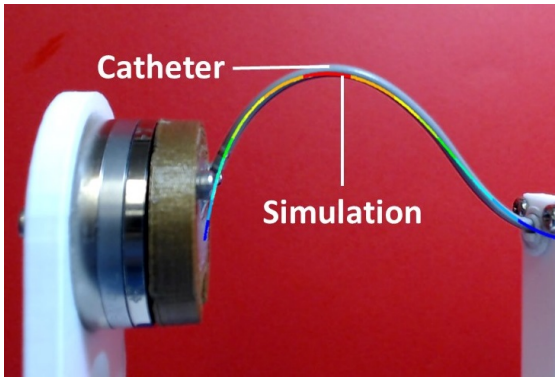

Fig. 6. Comparison of FEM simulation and experimental deformation for the tip of catheter when the catheter squeezed 40 mm to the force sensor.

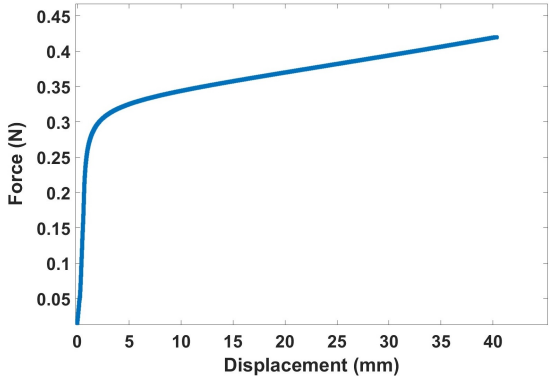

Fig. 7. Recorded force during the experiment when the tip of the catheter was squeezed for 40 mm.

TABLE II
MECHANICAL PROPERTIES OF CATHETER FOUND USING THE RSO.

Young's modulus (MPa)	Poisson ratio	Density (kg/m^3)
137.6	0.394	7736

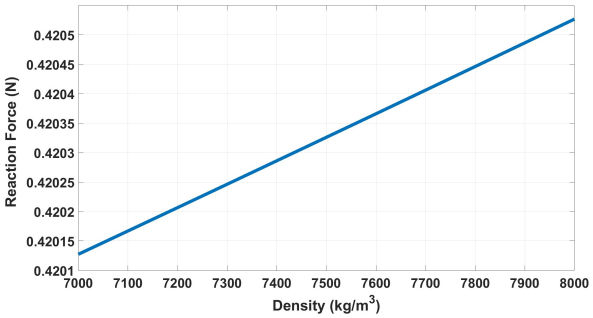

Fig. 8. Variation of reaction force by changing the density in the range of 7000 to 8000 (kg/m^3) while Young's modulus and Poisson's ratio are set to candidate values.

the RSO. The candidate points are the selected values of Young's modulus, Poisson's ratio, and density from I that satisfied the 0.4 N reaction force with 40 mm tip displacement. Figure 8 shows the variation of reaction force by changing the density in the range of 7000 to 8000 (kg/m^3) while Young's modulus and Poisson's ratio are set to 137.6 MPa and 0.394, respectively. Similarly, Figure 9 and Figure 10 show the variation of reaction force by changing the Young's modulus and Poisson ratio while other parameters are set to the candidate values. The Figures showed the sensitivity of the reaction force to the Young's modulus and Poisson ratio.

As illustrated in Figures 8 and 10, the reaction force is slightly changed by the variation of the density and Poisson's ratio. However, as shown in Figure 9 the reaction force is highly dependent on the value of Young's modulus. In addition, igures 11 to 13 provide a 3D plot of the variation in reaction force at the selected candidate points. The results showed that the reaction force increased by incensing Young's modulus and density. The reason for this is that the capability

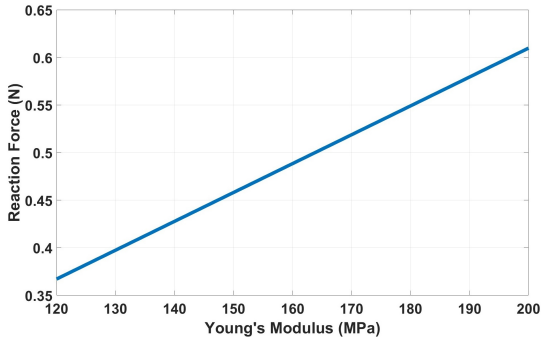

Fig. 9. Variation of reaction force by changing the Young's modulus in the range of 120 to 200 MPa while density and Poisson's ratio are set to candidate values.

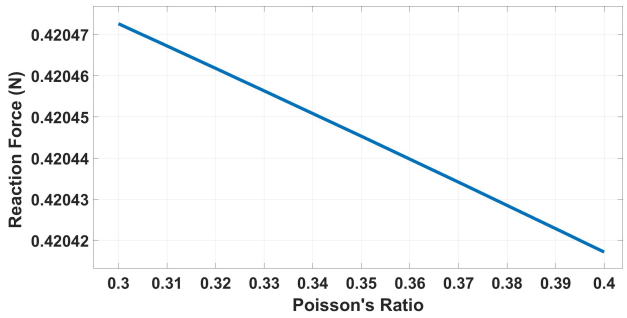

Fig. 10. Variation of reaction force by changing the Poisson's ratio in the range of 0.3 to 0.4 while Young's modulus and density are set to candidate values.

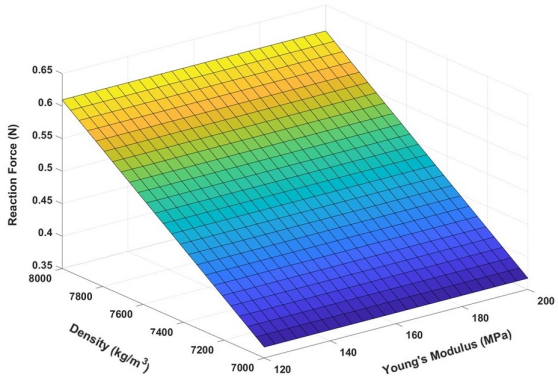

Fig. 11. Variation of reaction force by changing the Young's modulus and density.

of transferring force is directly related to the material property, and that by increasing the material property and having a stiffer material, more force can be transferred. However, by increasing the Poisson's ratio, the reaction force decreased. Moreover, as the catheter's tip weight is small, density almost has no impact on the reaction force, proving the validity of the quasi-statistics assumption in the FEM modeling and in the applications that the velocity of deformation is slow.

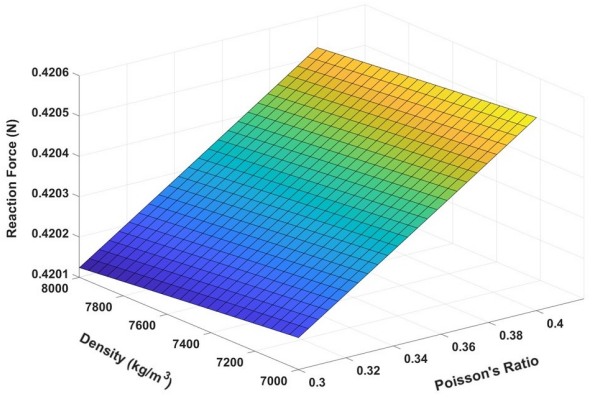

Fig. 12. Variation of reaction force by changing the Poisson's ratio and density.

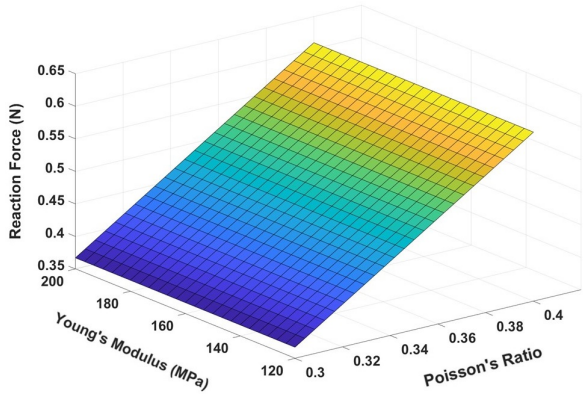

Fig. 13. Variation of reaction force by changing the Poisson's ratio and Young's modulus.

V. Conclusion And Future Work

A real-time force estimator is necessary for ensuring the safety and effectiveness of robot-assisted radio frequency ablation. The purpose of this study was to simulate a parametric finite element model for a steerable catheter which will be used for the estimation of force during radio frequency ablation procedures. A setup experiment is conducted to determine the design parameters of the catheter by comparing the deformation of the catheter between the experiment (by capturing the deformation of the catheter) and the finite element simulations. The results of the FE simulation were in fair agreement with the reference values obtained from the experiment. Based on the outcome of the current study, the proposed method was able to meet both the accuracy and speed requirements for procedures involving robot-assisted autonomous cardiac ablation. In terms of simulation speed, the time required for the ablation process to be completed can be measured and compared against a desired time frame or benchmark. For future work, a learning-from-simulation model will be proposed to estimate the tip contact force without actually running the simulation in real-time. This feature will enhance the accuracy and precision of minimally invasive procedures for robotic catheter intervention systems.

Acknowledgment

This research was supported by the Natural Science and Engineering Research Council (NSERC) of Canada through the NSERC CREATE Grant for Innovation-at-the-Cutting-Edge (ICE), the Fonds de Recherche du Quebec pour la Nature et les Technologies (FRQNT), Concordia University, and McGill University, Montreal, Quebec, Canada.

References

[1] G. F. Romiti et al., "Adherence to the 'atrial fibrillation better care'pathway in patients with atrial fibrillation: impact on clinical outcomes—a systematic review and meta-analysis of 285,000 patients," Thrombosis and haemostasis, vol. 122, no. 03, pp. 406–414, 2022.

[2] K. G. Graves et al., "Atrial fibrillation ablation and its impact on stroke," Current treatment options in cardiovascular medicine, vol. 20, no. 1, pp. 1–12, 2018.

[3] A. Hooshiar, S. Najarian, and J. Dargahi, "Haptic telerobotic cardiovascular intervention: a review of approaches, methods, and future perspectives," IEEE reviews in biomedical engineering, vol. 13, pp. 32–50, 2019.

[4] M. Runciman, A. Darzi, and G. P. Mylonas, "Soft robotics in minimally invasive surgery," Soft robotics, vol. 6, no. 4, pp. 423–443, 2019.

[5] N. Bandari, J. Dargahi, and M. Packirisamy, "Tactile sensors for minimally invasive surgery: A review of the state-of-the-art, applications, and perspectives," Ieee Access, vol. 8, pp. 7682–7708, 2019.

[6] N. M. Bandari, A. Hooshair, M. Packirisamy, and J. Dargahi, "Optical fiber array sensor for lateral and circumferential force measurement suitable for minimally invasive surgery: Design, modeling and analysis," in Specialty Optical Fibers. Optica Publishing Group, 2016.

[7] A. Sayadi, H. R. Nourani, M. Jolaei, J. Dargahi, and A. Hooshiar, "Force estimation on steerable catheters through learning-from-simulation with ex-vivo validation," in 2021 International Symposium on Medical Robotics (ISMR). IEEE, 2021, pp. 1–6.

[8] T. Torkaman, M. Roshanfar, J. Dargahi, and A. Hooshiar, "Embedded six-dof force-torque sensor for soft robots with learning-based calibration," IEEE Sensors Journal, 2023.

[9] T. Torkaman, M. Roshanfar, J. Dargahi, and A. Hooshiar, "Accurate embedded force sensor for soft robots with rate-dependent deep neural calibration," in 2022 IEEE International Symposium on Robotic and Sensors Environments (ROSE). IEEE, 2022, pp. 1–7.

[10] T. Torkaman, M. Roshanfar, J. Dargahi, and A. Hooshiar, "Analytical modeling and experimental validation of a gelatin-based shape sensor for soft robots," in 2022 International Symposium on Medical Robotics (ISMR). IEEE, 2022, pp. 1–7.

[11] L. Zou, C. Ge, Z. J. Wang, E. Cretu, and X. Li, "Novel tactile sensor technology and smart tactile sensing systems: A review," Sensors, vol. 17, no. 11, p. 2653, 2017.

[12] A. Hooshiar, N. M. Bandari, and J. Dargahi, "Image-based estimation of contact forces on catheters for robot-assisted cardiovascular intervention," in Hamlyn Symposium on Medical Robotics, 2018, pp. 119–120.

[13] M. Khoshnam and R. V. Patel, "Estimating contact force for steerable ablation catheters based on shape analysis," in 2014 IEEE/RSJ International Conference on Intelligent Robots and Systems. IEEE, 2014, pp. 3509–3514.

[14] A. Molaei, A. G. Aghdam, and J. Dargahi, "A versatile pseudo-rigid body modeling method," arXiv preprint arXiv:2206.06237, 2022.

[15] M. Jolaeimoghaddam, S. A. H. Ahmedi, and J. Dargahi, "Sensor-free force and position control of tendon-driven catheters through interaction modeling," Jul. 14 2022, uS Patent App. 17/647,673.

[16] S. Hasanzadeh and F. Janabi-Sharifi, "Model-based force estimation for intracardiac catheters," IEEE/ASME Transactions on Mechatronics, vol. 21, no. 1, pp. 154–162, 2015.

[17] M. Jolaei, A. Hooshiar, J. Dargahi, and M. Packirisamy, "Toward task autonomy in robotic cardiac ablation: Learning-based kinematic control of soft tendon-driven catheters," Soft Robotics, vol. 8, no. 3, pp. 340–351, 2021.

[18] M. Luo, H. Xie, L. Xie, P. Cai, and L. Gu, "A robust and real-time vascular intervention simulation based on kirchhoff elastic rod," Computerized medical imaging and graphics, vol. 38, no. 8, pp. 735–743, 2014.

[19] M. Roshanfar, A. Sayadi, J. Dargahi, and A. Hooshiar, "Stiffness adaptation of a hybrid soft surgical robot for improved safety in interventional surgery," in 2022 44th Annual International Conference of the IEEE Engineering in Medicine & Biology Society (EMBC). IEEE, 2022, pp. 4853–4859.

[20] M. Roshanfar, J. Dargahi, and A. Hooshiar, "Toward semi-autonomous stiffness adaptation of pneumatic soft robots: Modeling and validation," in 2021 IEEE International Conference on Autonomous Systems (ICAS). IEEE, 2021, pp. 1–5.

[21] P. Fekri et al., "Y-net: A deep convolutional architecture for 3d estimation of contact forces in intracardiac catheters," IEEE Robotics and Automation Letters, vol. 7, no. 2, pp. 3592–3599, 2022.

[22] P. Fekri et al., "A deep learning force estimator system for intracardiac catheters," 2021 IEEE International Symposium on Medical Measurements and Applications (MeMeA), vol. 7, no. 2, pp. 1–6, 2021.

[23] Boston Scientific, "Blazer XP temperature ablation catheter family," shorturl.at/bpszM, 2023.

[24] ATI Industrial Automation, "ATI multi-axis force/torque sensor, mini40," shorturl.at/bDKSZ, 2023.

 ISBN: 978-1-68558-053-7